Observation of Deep Occultation Signals in Tropical Cyclones With COSMIC-2 Measurements

Paweł Hordyniec, Yuriy Kuleshov, Suelynn Choy, and Robert Norman

***Abstract*—Global navigation satellite system (GNSS) signals in the radio occultation (RO) technique using new measurements from constellation observing system for meteorology, ionosphere & climate (COSMIC-2) mission were observed very deep below the Earth's limb. Selected occultations collocated with severe tropical cyclones showed the existence of signal-to-noise ratio (SNR) variations at or below −200 km in terms of height of straight line (HSL) connecting a pair of occulting satellites. The presence of such signals is considered as indicative of sharp inversion layers associated with planetary boundary layer. We investigate the potential application of deep occultation signals for detection of tropical cyclones often resulting in strong vertical gradients of refractivity. The most prominent deep signatures computed using 1 s running mean filter can reach 400 V/V, whereas the majority of deep signals exceed the noise level by a factor of two. The cross-satellite interference is important mechanism affecting the structure of deep signals, especially for global positioning system (GPS) occultations.**

***Index Terms*—Amplitude, deep signal, radio occultation (RO), tropical cyclone (TC).**

I. Introduction

TROPICAL cyclone (TC) monitoring and forecasting are important and challenging tasks as they require to promptly detect their intensification and issue early warnings in order to reduce impacts on communities at risk. One of the most detailed observations describing complicated vertical structures associated with TCs are gathered by global positioning system (GPS) dropsondes in reconnaissance aircraft missions [1]. Because low-pressure systems originate from oceanic regions, where *in situ* measurements mostly remain unavailable, their monitoring heavily relies on remote sensing satellite data [2], [3]. The recently launched constellation of six low Earth orbiting (LEO) satellites of the constellation observing system for meteorology, ionosphere & climate (COSMIC-2) mission [4] utilize very favorable configuration for collecting atmospheric profiles of the tropical troposphere due to equatorial orbital planes. Fundamental geophysical variables are derived from inversion of Doppler frequency shifts, which in geometrical optics do not require amplitude data. The amplitude expressed in terms of signal-to-noise ratio (SNR), serving mostly as a data-quality measure, can be also a valuable indicator of atmospheric variability such as deep fading amplitude in the presence of super-refractions [5] associated with sharp inversion layers [6] or ionospheric gradients and irregularities induced by sporadic E layers [7]. Ding *et al.* [8] present the evidence of strong vertical gradients in the vicinity of TCs suggesting pronounced planetary boundary layer. Fig. 1 shows the example of refractivity structures modeled from dropsonde released in the eyewall of tropical storm Nestor. The so-called tropospheric ducts are recognized by inducing anomalous

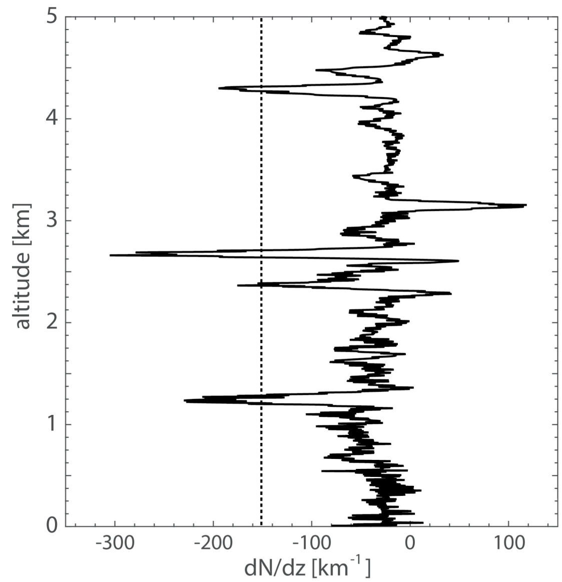

Fig. 1. Vertical gradient of refractivity with multiple super-refraction layers (dN/dz ≤ -157) modeled from high-resolution dropsonde profile collected on 19 October 2019 in the vicinity of tropical storm Nestor. The threshold value of -157 is marked with dashed line.

Manuscript received January 9, 2021; revised April 27, 2021 and June 1, 2021; accepted June 15, 2021. Date of publication July 12, 2021; date of current version December 15, 2021. This work was supported by the Australian Antarctic Science Grant Program Project 4469. Robert Norman is supported by the Cooperative Research Centre for Space Environment Management (SERC Limited) through the Australian Government's Cooperative Research Centre Program. *(Corresponding author: Paweł Hordyniec.)*

Paweł Hordyniec is with the SPACE Research Centre, RMIT University, Melbourne, VIC 3000, Australia, and also with the Institute of Geodesy and Geoinformatics, Wrocław University of Environmental and Life Sciences, 50-375 Wrocław, Poland (e-mail: pawel.hordyniec@upwr.edu.pl).

Yuriy Kuleshov is with the Bureau of Meteorology, Melbourne, VIC 3008, Australia, also with the SPACE Research Centre, RMIT University, Melbourne, VIC 3000, Australia, and also with the School of Mathematics and Statistics, The University of Melbourne, Melbourne, VIC 3010, Australia (e-mail: yuriy.kuleshov@bom.gov.au).

Suelynn Choy is with the SPACE Research Centre, RMIT University, Melbourne, VIC 3000, Australia (e-mail: suelynn.choy@rmit.edu.au).

Robert Norman is with the SERC Limited, Mount Stromlo Observatory, Weston Creek, ACT 2611, Australia (e-mail: robert.norman7@gmail.com).

Digital Object Identifier 10.1109/LGRS.2021.3092511

propagation of radio signals resulting in negatively biased radio occultation (RO) retrievals of refractivity because of ill-conditioned inversions [9]. Tropospheric ducts can result in a diffraction mechanism producing signatures in the signal's amplitude observed when the occulting satellite is in the very deep Earth's shadow [10]. The signatures can often appear below the minimum height of straight line (HSL) connecting global navigation satellite system (GNSS) and LEO satellites (−200 km) typically tracked by LEO receivers imposed by channel limitations. Improvements made in development of new generation RO receivers placed on-board COSMIC-2 satellites contributed to increased SNR allowing for more reliable tracking of deep signals. In the following study, amplitudes observed with one LEO satellite of COSMIC-2 constellation set to track signals down to very low HSL are studied to find potential correspondence to atmospheric conditions associated with TCs. We establish collocations of RO events with severe TCs and perform spectral analysis of observed signals. The statistical significance of deep signals induced by super-refraction layers is evaluated relative to various RO tunable parameters.

II. Data and Methods

A. COSMIC-2 Occultations

COSMIC-2 satellites in the period between 30 October and 9 December in 2019 occasionally tracked the signal down to the lowest HSL < −350 km. These measurements were recorded by the LEO spacecraft #E1 (RO products with C2E1 in occultation IDs) in setting occultations. All other flight modules typically tracked the signal down to lowest HSL of −200 km. In total 9552 occultations to LEO satellite #E1 propagated deeper than −200 km, while 8645 events reached HSL below −350 km. The excess Doppler (phase) and SNR (amplitude) data are obtained from FORMOSAT-7/COSMIC-2 Neutral Atmospheric Provisional Release 1. The provided (original) SNR values are scaled by a factor of ten.[1] The independent variable of straight line tangent altitude (HSL) describes the propagation depth of RO signals

$$\mathrm{HSL} = \frac{r_L r_G \sin\theta}{\sqrt{r_L^2 + r_G^2 - 2 r_L r_G \cos\theta}} - r_e \tag{1}$$

where r_e is local radius of curvature, θ is the central angle between radii r_L, and r_G for LEO and GNSS positions at given observation epoch. Following tunable RO parameters together with respective SNR values are analyzed: 1) lowest (bottom) HSL for which the phase and amplitude data are available; 2) HSL at the SNR cut-off point; and 3) HSL for the Doppler cut-off point. For the identification of deep signatures the SNR is averaged from 100 to 1 Hz by applying running mean filter to reduce the impact of noise. The deep signals can be considered statistically significant if their magnitudes exceed the noise level defined as the lowest voltage SNR in 1-Hz running mean data. In RO retrieval methodologies, signals

[1]For more details see https://cdaac-www.cosmic.ucar.edu/cdaac/doc/documents/snr.pdf

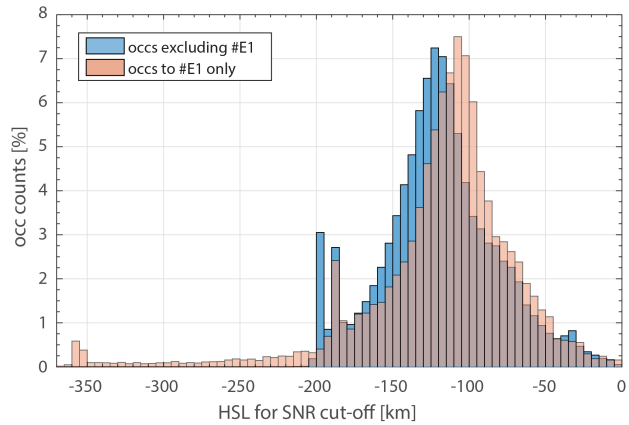

Fig. 2. Distribution of HSL for SNR cut-off showing (orange) potential deep signatures from occultations to spacecraft #E1 and (blue) no signals below −200 km from observations to other satellites.

observed down to HSL of SNR cut-off are inverted to neutral atmosphere profiles. Failure to include deep tropospheric signals may result in inversion biases [11]. We search for deep signals based on daily statistics computed from one sigma-filtered HSLs for SNR cut-off points. The mean SNR cut-off altitude for the study period is on the order of −120-km HSL with the lowest minimum varying around −160 km (threshold for deep signals detection). Fig. 2 shows that in total 14% of #E1 occultations (2530 observations) contain potential contributions from deep signals (HSL < −160 km), with 2% spikes in data counts at −200-km HSL for both deep tracking and typical occultations.

B. Collocations With Tropical Cyclones

Data for TCs observed in the period from October 2019 to April 2020 are retrieved from International Best Track Archive for Climate Stewardship (IBTrACS) [12]. The distribution of TC tracks in 3-h temporal resolution is presented in Fig. 3. Collocated COSMIC-2 occultations satisfy the temporal and spatial criteria of ±2 h difference and up to 600-km distance mismatch, respectively. The analysis of amplitude signals is restricted to deep occultations in the vicinity of Category 1 or higher in terms of the Saffir–Simpson hurricane wind scale. The identified cases are listed in Table I. Well-matched intersections of occultation planes with TC paths can be selected based on the azimuth computed between collocated pairs of TC location and COSMIC-2 tangent point. The azimuth difference of 0° (360°) or 180° corresponds to the occultation plane being perpendicular to the TC track with GNSS signals propagating through the central eye. This criterion is important for collocations having a mismatch distance larger than diameter of TC eye and its outer eyewall. According to [13], the mean eye radius is 26 km, whereas the size of TCs for the large-eye class can exceed 100 km. The eyewall sizes appear to be proportional to the eye size with the average of the order of 50 km [14]. These values should be contrasted with a mean horizontal resolution of the RO technique of about 300 km in the troposphere further extending the observation radius for nearest collocations.

TABLE I

COLLOCATIONS OF TCs WITH COSMIC-2 CHARACTERIZED BY VERY LOW HSL AT THE BOTTOM OF OCCULTATION (* REFERS TO OCCULTATIONS WITH MORE THAN ONE COLLOCATION)

No.	Name	Lat [deg]	Lon [deg]	Cat.	ΔTime [min]	Distance [km]	ΔAzimuth [deg]	Occultation ID IIII.YYYY.DDD.HH.MM.GGG	HSLBOT [km]
#1	KYARR	19.05	61.55	1	52	507.28	114.43	C2E1.2019.303.08.08.G22	-358.91
#2	HALONG	18.70	152.30	3	-106	579.97	8.09	*C2E1.2019.308.19.46.G06	-357.27
#3	HALONG	22.05	150.89	4	-67	361.59	264.48	*C2E1.2019.310.16.07.G09	-359.09
#4	HALONG	24.95	152.44	2	-59	172.50	292.03	C2E1.2019.311.15.59.G09	-360.28
#5	MATMO	16.90	87.50	1	91	574.05	257.28	C2E1.2019.311.22.29.R18	-359.30
#6	NAKRI	12.90	115.30	1	39	102.24	335.38	C2E1.2019.312.17.21.G19	-356.95
#7	FENGSHEN	25.80	146.80	3	44	563.32	277.77	C2E1.2019.320.11.16.G22	-357.81
#8	FENGSHEN	26.70	149.30	3	1	339.00	33.71	C2E1.2019.320.17.59.R14	-356.38
#9	KAMMURI	12.80	138.50	1	-108	294.08	79.38	*C2E1.2019.332.07.48.R14	-257.17
#10	KAMMURI	14.60	137.60	1	3	536.37	304.73	C2E1.2019.333.05.57.R17	-358.41
#11	KAMMURI	14.10	137.90	1	56	98.34	92.79	C2E1.2019.333.11.04.G03	-358.04
#12	KAMMURI	14.06	137.68	1	34	509.82	164.80	C2E1.2019.333.14.26.R09	-355.80
#13	KAMMURI	13.60	135.20	1	11	450.28	259.22	C2E1.2019.334.05.49.R18	-359.85
#14	KAMMURI	13.01	125.18	3	-96	583.73	145.60	C2E1.2019.336.10.36.R11	-306.94
#15	AMBALI	-10.21	62.28	4	-46	594.04	272.48	C2E1.2019.339.21.46.G29	-354.32
#16	AMBALI	-10.50	62.20	4	-73	484.06	184.58	*C2E1.2019.340.01.13.G31	-358.75
#17	BELNA	-8.97	48.46	1	15	343.63	348.87	C2E1.2019.340.14.45.R11	-357.32
#18	BELNA	-9.20	48.40	1	-12	395.02	220.49	C2E1.2019.340.18.12.G12	-357.74
#19	BELNA	-9.23	47.67	1	20	532.60	36.83	C2E1.2019.341.02.40.G22	-358.42
#20	BELNA	-10.58	47.34	3	23	262.13	81.67	C2E1.2019.341.14.37.R12	-407.00
#21	BELNA	-10.90	47.20	3	-3	432.76	222.13	C2E1.2019.341.18.03.G12	-360.36
#22	BELNA	-10.90	47.20	3	-3	491.26	130.25	C2E1.2019.341.18.03.R02	-358.37
#23	BELNA	-11.94	46.56	2	29	257.00	346.39	C2E1.2019.342.02.31.G22	-358.06
#24	BELNA	-12.90	46.30	2	6	474.04	229.09	C2E1.2019.342.17.54.G12	-358.26
#25	BELNA	-12.90	46.30	2	6	273.83	150.50	C2E1.2019.342.17.54.R03	-359.66
#26	BELNA	-13.60	46.00	1	60	303.28	221.18	*C2E1.2019.342.23.00.R19	-359.48

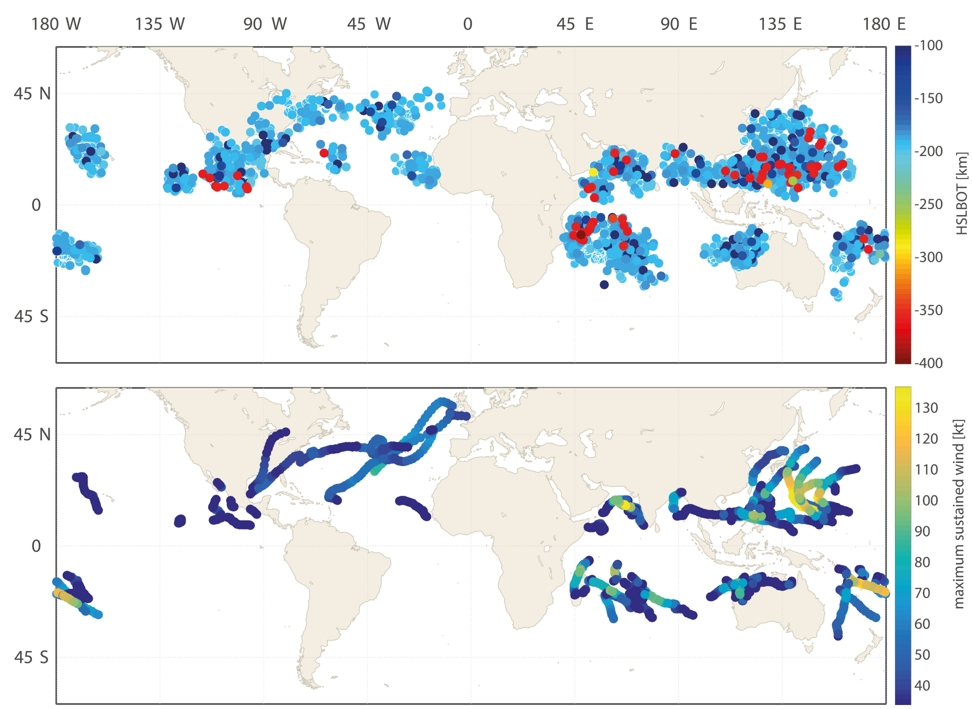

Fig. 3. Distribution of (top) collocated COSMIC-2 measurements with (bottom) TCs observed between October 2019 and April 2020.

III. COSMIC-2 DEEP SIGNALS IN TROPICAL CYCLONES

The spatial spectra in HSL-frequency domain presented in Fig. 4 are computed according to [15] using phase observations from conPhs format with applied GPS navigation modulation bits [16], thus their external removal is not required. The mismatch distance of occultation #3 to Category 4 TC is comparable to the horizontal resolution of RO measurements suggesting possible interaction of signals with the outer eyewall. However, the noisy spectra shows only weak signals below −200-km HSL. Detailed analysis of spectrograms for event #11 revealed interference from other nonocculting satellite being another possible source of deep signals [10], which is visible as cross-line pattern at −200-km HSL, coinciding with 400 V/V spike in averaged SNR. The prominent deep signals were observed with occultation #16. The spectrogram

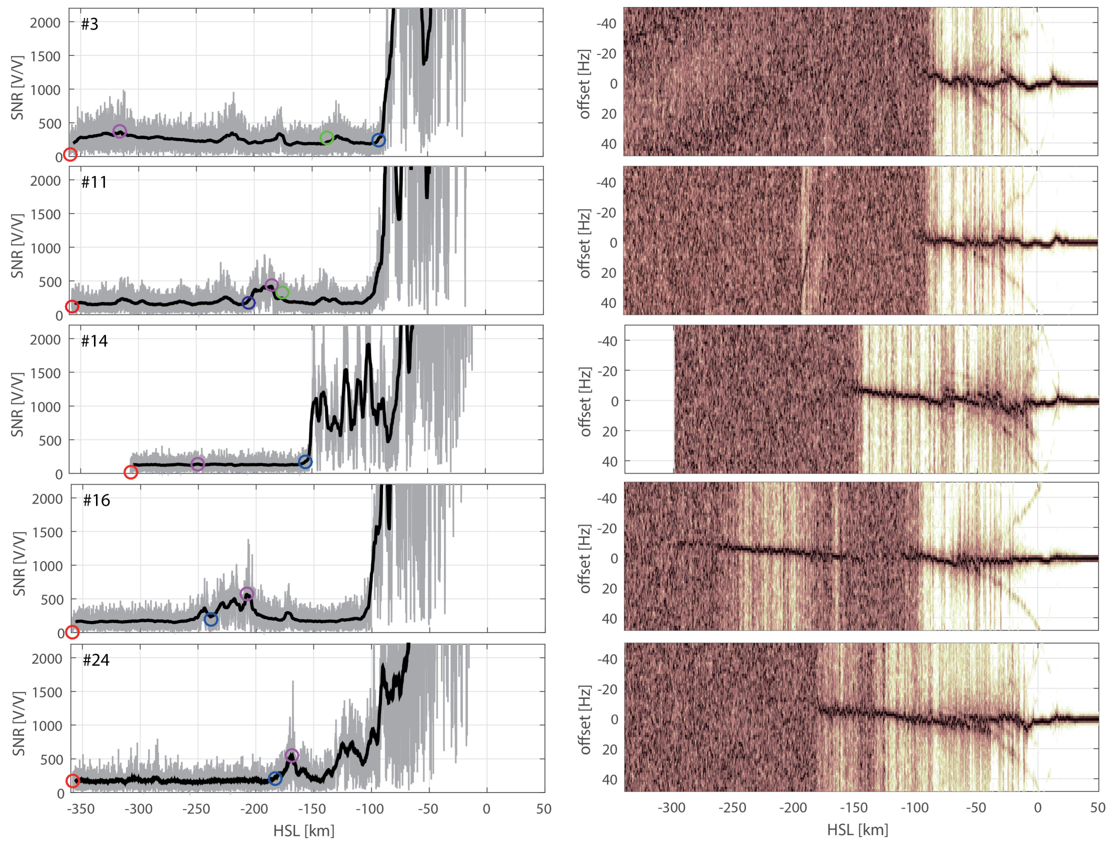

Fig. 4. Deep occultation signals from collocations with TCs. (Left panels) SNRs as a function of HSL. The strongest deep amplitudes are marked with purple circles, while other tunable RO parameters correspond to SNR cut-off (blue), Doppler cut-off (green), and lowermost straight-line tangent altitude (red). (Right panels) sliding spectrograms showing frequency offset computed between observed Doppler and phase model.

clearly supports the evidence of tropospheric propagation between −200- to −250-km HSL. The signal observed in the event #24 might not be necessary regarded as a deep signature because the SNR re-emerges shortly after reaching the noise level at around −150-km HSL. If we on other hand define deep signals as amplitudes observed below the noise boundary in the spectrograms, the mean SNR above 500 V/V should be regarded as statistically significant. All above discussed cases were recorded by GPS occulting satellites. Generally, no deep signals were observed in Globalnaja Nawigacionnaja Sputnikowaja Sistiema (GLONASS) occultations. One particular case discussed here is the event #14 shown in Fig. 4 to demonstrate structure of direct and strong signals tracked down to −150-km HSL. Fig. 5 shows voltage SNR with corresponding HSL of deep occultations and the magnitude of refractivity gradients collocated with the TCs. It can be seen that some signals extend below the SNR cut-off point of −200-km HSL (#11, #17) down to −240 km (#16). With SNR exceeding 568 V/V the occultation #16 shows the strongest signature amongst identified collocations. The spikes in 100-Hz SNR data visible in Fig. 4 exceed 1000 V/V at HSL corresponding to the largest deep amplitudes computed in 1-s interval of running mean. However, refractivity gradients based on COSMIC-2 and European Centre for Medium-Range Weather Forecasts (ECMWF) data for occultation #16 do not show the evidence of ducting layers. On the contrary, the most significant dN/dz values from ECMWF exceeding $-157\ \text{km}^{-1}$ for #8 and #14 are not reflected in deep signals. For the case #24, the magnitude of dN/dz is close to critical, which may explain signals below −150-km HSL in Fig. 4. The gradients observed with COSMIC-2 typically correspond to standard refractive conditions with the average of $-80\ \text{km}^{-1}$. The noise level for GPS occultations is on average ∼150 V/V, while ∼115 V/V for GLONASS. The larger noise in GPS data might be induced by cross-satellite interference, which does not affect GLONASS that uses frequency division multiple access (FDMA). After exclusion of occultations with strong interfering signals (#2, #11), the magnitude of GPS deep amplitudes is on average two times larger than the noise level. The weakest deep signal is found in occultation #1 (20% larger than noise), whereas nearly four times larger deep SNR relative to the noise is observed with occultation #16. As it can be clearly seen in Fig. 5, GLONASS signals are very comparable to the noise level suggesting no deep signals.

IV. Summary and Discussion

COSMIC-2 occultations collocated with TCs were analyzed in terms of occurrence of deep signatures in the amplitude data. Although few spectrograms showed clear signals at or below −200-km HSL, most of deep signals were difficult to visually distinguish from the noise in the computed Doppler frequency offset. The existence of deep signals can be inferred from the analysis of refractivity. However, COSMIC-2 generally shows substantially underestimated refractivity gradients relative to ECMWF or dropsondes. Because deep occultations

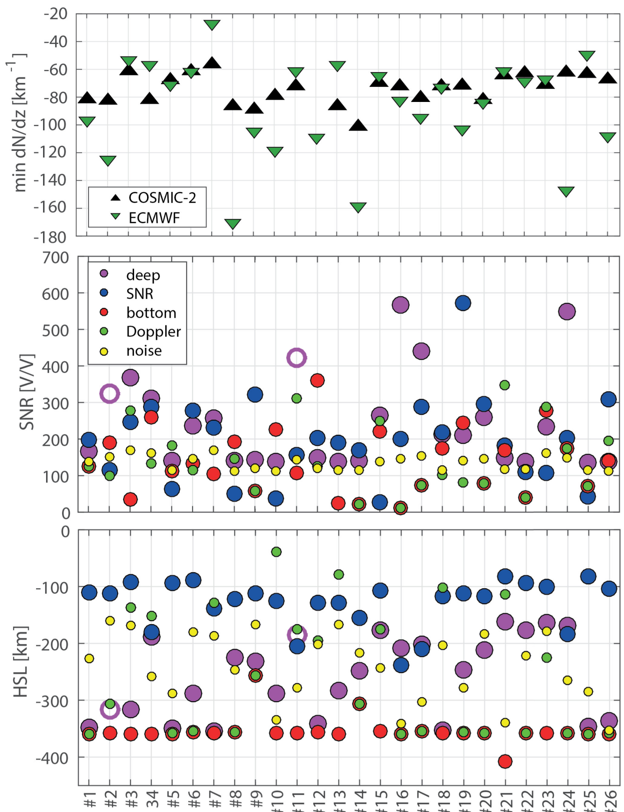

Fig. 5. Distribution of (top) refractivity gradients and (middle) SNR values with (bottom) corresponding HSL for the strongest deep signals (purple) found in collocations with TCs. Other tunable RO parameters represent: SNR cut-off (blue), Doppler cut-off (green), and lowermost HSL (red). The noise level is marked with yellow dots. The purple circles indicate deep amplitudes due to clear interfering signals. The out-of-scale SNR values for occultations #7, #10, and #13 corresponding to Doppler cut-offs have magnitudes of 1989, 5254, and 1047 V/V, respectively.

were identified in the presence of standard refraction in COSMIC-2 and no deep signals were found in occultations collocated with critical gradients in ECMWF, the connection between ducting and deep RO signals is to be confirmed. The cross-satellite interference in GPS occultations is a major disturbing factor altering the structure of observed signals. Detailed data analysis supports the evidence that the magnitude of deep signals can be overshadowed by the interfering signals. However, discussion and demonstration of possible mechanisms is not possible with the data used in the study and additional scientific efforts are required. Variations in the running mean SNR of 367 and 567 V/V (with spikes reaching ∼1000 and ∼1500 V/V in 100-Hz data) were amongst the most statistically significant deep signals induced by propagation through Category 4 TCs. Deep tracking RO data can be used in TC analysis to obtain information about interaction between a cyclone and ambient environment which is generally hostile to duct formation. However, strong ducts exist: 1) inside the TC circulations associated with successive subsidence in the gaps among the spiral cloud bands and 2) in the transition zone between TCs and ambient environment impacted by inflow of dry and cold air or subsidence inversion. The peak Atlantic hurricane season of 2020 constitutes the first complete year for studying TCs with new generation RO signals to support the presented results.

Acknowledgment

The authors would like to thank UCAR/CDAAC for providing access to COSMIC-2 provisional dataset available at https://data.cosmic.ucar.edu/gnss-ro/cosmic2/provisional/. Tropical cyclone data were downloaded from https://www.ncdc.noaa.gov/ibtracs/.

References

[1] J. Wang *et al.*, "A long-term, high-quality, high-vertical-resolution GPS dropsonde dataset for hurricane and other studies," *Bull. Amer. Meteorological Soc.*, vol. 96, no. 6, pp. 961–973, Jun. 2015.

[2] C. Velden *et al.*, "The Dvorak tropical cyclone intensity estimation technique: A satellite-based method that has endured for over 30 years," *Bull. Amer. Meteorological Soc.*, vol. 87, no. 9, pp. 1195–1210, Sep. 2006.

[3] P. Vergados, Z. J. Luo, K. Emanuel, and A. J. Mannucci, "Observational tests of hurricane intensity estimations using GPS radio occultations," *J. Geophys. Res., Atmos.*, vol. 119, no. 4, pp. 1936–1948, Feb. 2014.

[4] W. S. Schreiner *et al.*, "Cosmic-2 radio occultation constellation: First results," *Geophys. Res. Lett.*, vol. 47, no. 4, 2020, Art. no. e2019GL086841.

[5] S. Sokolovskiy, "Effect of superrefraction on inversions of radio occultation signals in the lower troposphere," *Radio Sci.*, vol. 38, no. 3, pp. 1–24, 2003.

[6] F. Xie, D. L. Wu, C. O. Ao, A. J. Mannucci, and E. R. Kursinski, "Advances and limitations of atmospheric boundary layer observations with GPS occultation over southeast Pacific ocean," *Atmos. Chem. Phys.*, vol. 12, no. 2, pp. 903–918, Jan. 2012.

[7] W.-H. Yeh, C.-Y. Huang, T.-Y. Hsiao, T.-C. Chiu, C.-H. Lin, and Y.-A. Liou, "Amplitude morphology of GPS radio occultation data for sporadic-E layers," *J. Geophys. Res. Space Phys.*, vol. 117, no. A11, pp. 1–8, 2012.

[8] J. Ding, J. Fei, X. Huang, X. Cheng, and X. Hu, "Observational occurrence of tropical cyclone ducts from Gps dropsonde data," *J. Appl. Meteorol. Climatol.*, vol. 52, no. 5, pp. 1221–1236, May 2013.

[9] C. O. Ao, T. Meehan, G. Hajj, A. Mannucci, and G. Beyerle, "Lower troposphere refractivity bias in GPS occultation retrievals," *J. Geophys. Res.*, vol. 108, no. D18, pp. 1–16, 2003.

[10] S. Sokolovskiy, W. Schreiner, Z. Zeng, D. Hunt, Y.-C. Lin, and Y.-H. Kuo, "Observation, analysis, and modeling of deep radio occultation signals: Effects of tropospheric ducts and interfering signals," *Radio Sci.*, vol. 49, no. 10, pp. 954–970, Oct. 2014.

[11] S. Sokolovskiy, C. Rocken, W. Schreiner, and D. Hunt, "On the uncertainty of radio occultation inversions in the lower troposphere," *J. Geophys. Res.*, vol. 115, no. D22, pp. 1–19, 2010.

[12] K. R. Knapp, M. C. Kruk, D. H. Levinson, H. J. Diamond, and C. J. Neumann, "The international best track archive for climate stewardship (IBTrACS): Unifying tropical cyclone data," *Bull. Amer. Meteorological Soc.*, vol. 91, no. 3, pp. 363–376, Mar. 2010.

[13] C. L. Weatherford and W. M. Gray, "Typhoon structure as revealed by aircraft reconnaissance. Part II: Structural variability," *Monthly Weather Rev.*, vol. 116, no. 5, pp. 1044–1056, May 1988.

[14] K. R. Knapp, C. S. Velden, and A. J. Wimmers, "A global climatology of tropical cyclone eyes," *Monthly Weather Rev.*, vol. 146, no. 7, pp. 2089–2101, Jul. 2018.

[15] M. E. Gorbunov, K. B. Lauritsen, A. Rhodin, M. Tomassini, and L. Kornblueh, "Radio holographic filtering, error estimation, and quality control of radio occultation data," *J. Geophys. Research: Atmos.*, vol. 111, no. D10, pp. 1–10, May 2006.

[16] S. Sokolovskiy, C. Rocken, W. Schreiner, D. Hunt, and J. Johnson, "Postprocessing of L_1 GPS radio occultation signals recorded in open-loop mode," *Radio Sci.*, vol. 44, no. 2, pp. 1–13, Apr. 2009.